

A Near Edge X-ray Absorption Fine Structure Spectroscopy Investigation of the Structure of Self-Assembled Films of Octadecyltrichlorosilane

Richard D. Peters, Paul F. Nealey,* Jason N. Crain, and Franz J. Himpsel

Department of Chemical Engineering and Center for Nanotechnology and Department of Physics, University of Wisconsin, Madison, Wisconsin 53706

Received July 30, 2001. In Final Form: November 15, 2001

Polarization-dependent near edge X-ray absorption fine structure (NEXAFS) spectroscopy was used to determine the ordering of octadecyltrichlorosilane (OTS) molecules in self-assembled (SA) films on Si/SiO₂. Coverages of adsorbed material for different SA films were determined by integration of the NEXAFS signal due entirely to the C 1s absorption. The structures and coverages of the SA films deposited by chemisorption from solution in toluene were determined for two different deposition conditions: (1) open to the atmosphere and (2) water- and oxygen-free conditions inside a drybox. SA films of OTS deposited under ambient air conditions grew as islands on the substrate and were well-ordered as indicated by a strong polarization-dependence in the NEXAFS spectra. For depositions performed in the drybox, ordered or disordered films grew uniformly over the substrate. Ordered SA films deposited in the drybox exhibited higher average tilt angles and lower coverages of adsorbed material than SA films deposited under ambient air conditions. The structure and coverage are discussed with respect to results from measurements of contact angles of water and ellipsometry.

Introduction

Self-assembled (SA) films of alkylsiloxanes have been studied for use as boundary lubricants,^{1–8} ultrathin imaging layers^{9–13} and resist materials^{14–19} for nanolithography, and adhesion promoters for biological applications.^{20–27} Several different techniques have been

used to deposit SA films of alkylsiloxanes including Langmuir–Blodgett,²⁸ chemical vapor deposition,²⁹ and solution techniques. The structure and properties of these films are sensitive to the deposition conditions, and this sensitivity poses challenges for reproducible determination of structure–property relationships.

The formation and structure of self-assembled monolayers (SAMs) of alkylsiloxanes, specifically SAMs of octadecyltrichlorosilane (OTS), deposited by the solution method have been studied extensively on various substrates and under different deposition conditions.^{30–45} A well-ordered SAM generally is considered to be close-

* To whom correspondence should be addressed. E-mail: nealey@engr.wisc.edu.

(1) Reiter, G.; Demirel, A. L.; Peanasky, J.; Cai, L. L.; Granick, S. *J. Chem. Phys.* **1994**, *101*, 2606.

(2) Xiao, X.; Hu, J.; Charych, D. H.; Salmeron, M. *Langmuir* **1996**, *12*, 235.

(3) Huang, J. Y.; Song, K. J.; Lagoutchev, A.; Yang, P. K.; Chuang, T. *J. Langmuir* **1997**, *13*, 58.

(4) Lee, B.-w.; Clark, N. A. *Langmuir* **1998**, *14*, 5495.

(5) Tian, F.; Xiao, X.; Loy, M. M. T. *Langmuir* **1999**, *15*, 244.

(6) Clear, S. C.; Nealey, P. F. *J. Colloid Interface Sci.* **1999**, *213*, 238.

(7) Clear, S. C.; Nealey, P. F. *Langmuir* **2001**, *17*, 720.

(8) Clear, S. C.; Nealey, P. F. *J. Chem. Phys.* **2001**, *114*, 2802.

(9) Peters, R. D.; Yang, X. M.; Wang, Q.; de Pablo, J. J.; Nealey, P. *J. Vac. Sci. Technol., B* **2000**, *18*, 3530.

(10) Yang, X. M.; Peters, R. D.; Nealey, P. F.; Solak, H. H.; Cerrina, F. *Macromolecules* **2000**, *33*, 9575.

(11) Yang, X. M.; Peters, R. D.; Kim, T. K.; Nealey, P. F.; Brandow, S. L.; Chen, M.-S.; Shirey, L. M.; Dressick, W. J. *Langmuir* **2001**, *17*, 228.

(12) Peters, R. D.; Yang, X. M.; Kim, T. K.; Sohn, B. H.; Nealey, P. F. *Langmuir* **2000**, *16*, 4625.

(13) Dressick, W. J.; Chen, M.-S.; Brandow, S. L.; Rhee, K. W.; Shirey, L. M.; Perkins, F. K. *Appl. Phys. Lett.* **2001**, *78*, 676.

(14) Lercel, M. J.; Rooks, M.; Tiberio, R. C.; Craighead, H. G.; Sheen, C. W.; Parikh, A. N.; Allara, D. L. *J. Vac. Sci. Technol., B* **1995**, *13*, 1139.

(15) Lercel, M. J.; Whelan, C. S.; Craighead, H. G.; Seshadri, K.; Allara, D. L. *J. Vac. Sci. Technol., B* **1996**, *14*, 4085.

(16) Lercel, M. J.; Craighead, H. G.; Parikh, A. N.; Seshadri, K.; Allara, D. L. *Appl. Phys. Lett.* **1996**, *68*, 1504.

(17) Carr, D. W.; Lercel, M. J.; Whelan, C. S.; Craighead, H. G.; Seshadri, K.; Allara, D. L. *J. Vac. Sci. Technol., A* **1997**, *15*, 1446.

(18) Hild, R.; David, C.; Muller, H. U.; Volkel, B.; Kayser, D. R.; Grunze, M. *Langmuir* **1998**, *14*, 342.

(19) Sugimura, H.; Ushiyama, K.; Hozumi, A.; Takai, O. *Langmuir* **2000**, *16*, 885.

(20) Matsuzawa, M.; Potember, R. S.; Stenger, D. A.; Krauthamer, V. *J. Neurosci. Methods* **1993**, *50*, 253.

(21) Healy, K. E.; Thomas, C. H.; Rezanian, A.; Kim, J. E.; McKeown, P. J.; Lom, B.; Hockberger, P. E. *Biomaterials* **1996**, *17*, 195.

(22) Rezanian, A.; Thomas, C. H.; Healy, K. E. *Ann. Biomed. Eng.* **1997**, *25*, 190.

(23) Petrash, S.; Sheller, N. B.; Dando, W.; Foster, M. D. *Langmuir* **1997**, *13*, 1881.

(24) Sheller, N. B.; Petrash, S.; Foster, M. D.; Tsukruk, V. V. *Langmuir* **1998**, *14*, 4535.

(25) Willner, I.; Schlittner, A.; Doron, A.; Joselevich, E. *Langmuir* **1999**, *15*, 2766.

(26) McFarland, C. D.; Thomas, C. H.; DeFilippis, C.; Steele, J. G.; Healy, K. E. *J. Biomed. Mater. Res.* **2000**, *49*, 200.

(27) Franco, M.; Nealey, P. F.; Campbell, S.; Teixeira, A. I.; Murphy, C. J. *J. Biomed. Mater. Res.* **2000**, *52*, 261.

(28) Kojio, K.; Takahara, A.; Omote, K.; Kajiyama, T. *Langmuir* **2000**, *16*, 3932.

(29) Ferguson, G. S.; Chaudhury, M. K.; Biebuyck, H. A.; Whitesides, G. M. *Macromolecules* **1993**, *26*, 5870.

(30) Wasserman, S. R.; Tao, Y. T.; Whitesides, G. M. *Langmuir* **1989**, *5*, 1074.

(31) Wasserman, S. R.; Whitesides, G. M.; Tidswell, I. M.; Ocko, B. M.; Pershan, P. S.; Axe, J. D. *J. Am. Chem. Soc.* **1989**, *111*, 5852.

(32) Tidswell, I. M.; Rabedeau, T. A.; Pershan, P. S.; Kosowsky, S. D.; Folkers, J. P.; Whitesides, G. M. *J. Chem. Phys.* **1991**, *95*, 2854.

(33) Angst, D. L.; Simmons, G. W. *Langmuir* **1991**, *7*, 2236.

(34) Silberzan, P.; Leger, L.; Aussere, D.; Benattar, J. *J. Langmuir* **1991**, *7*, 1647.

(35) Schwartz, D. K.; Steinberg, S.; Israelachvili, J.; Zasadzinski, J. A. N. *Phys. Rev. Lett.* **1992**, *69*, 3354.

(36) Lefrange, J. D.; Markham, J. L.; Kurkjian, C. R. *Langmuir* **1993**, *9*, 1749.

(37) Parikh, A. N.; Allara, D. L.; Ben Azouz, I.; Rondelez, F. *J. Phys. Chem.* **1994**, *98*, 7577.

(38) Brzoska, J. B.; Ben Azouz, I.; Rondelez, F. *Langmuir* **1994**, *10*, 4367.

(39) Allara, D. L.; Parikh, A. N.; Rondelez, F. *Langmuir* **1995**, *11*, 2357.

packed and quasi-crystalline with monolayer thickness corresponding to fully extended chains.⁴⁶ In this configuration for OTS, the chemisorbed chains are in an all-trans conformation with an average tilt angle $\leq 15^\circ$ away from the surface normal.⁴⁶ Two mechanisms of growth are described in the literature. In the mechanism known as the "uniform" model, silane molecules initially are distributed homogeneously over the substrate in a disordered, liquidlike manner.^{31–33,40} The average tilt angle of the adsorbed chains is greater than 15° because of lower packing densities and gauche conformations for the chains. With increasing coverage, the disordered film is transformed into a densely packed, quasi-crystalline structure. In the mechanism known as the "island" model, domains of well-ordered, fully extended OTS molecules are heterogeneously grown on the substrate, and these domains are separated by uncovered regions of the substrate.^{35,37,42,47} These islands typically have dimensions on the order of hundreds of nanometers. With increasing deposition time, more domains are adsorbed until complete coverage of the substrate is achieved.

One of the challenges in using SA films of OTS is the difficulty in depositing films with reproducible structures and properties. Several key experimental conditions have been found to affect the structure and growth of the SA films of OTS: (1) deposition temperature, (2) substrate surface properties, and (3) concentration of water in the silane solution. Several groups have shown that the deposition temperature, T , has an effect on the structure of SA films.^{37,38,48–50} For depositions performed below a critical temperature, T_c , the SA films grow following the island model and are well-ordered with an all-trans conformation and monolayer thickness. For $T > T_c$, the SA films become partially disordered with decreased coverage of alkyl chains and increased gauche conformations compared to complete SAMs. Brzoska et al. proposed a mechanism to explain this temperature dependence.³⁸ An ultrathin interfacial film of water exists at the substrate onto which the alkyl chains adsorb in a Langmuir-like monolayer. This water catalyzes hydrolysis of the chlorosilanes and gives mobility to the adsorbed chains. Below T_c , the adsorption process occurs from a gaslike phase, while above T_c , the adsorption occurs from a denser phase that creates a thermodynamic barrier to adsorption.

The mechanism proposed by Brzoska et al. depends on the surface properties of the substrate, specifically, the hydration of the substrate. Several groups have shown that substrate surface properties such as concentration of OH groups and hydration can affect the growth of the SA films of OTS.^{33,36,39–41,43,51} Angst et al. showed that films of OTS on nonhydrated SiO_2 were less ordered than

films of OTS deposited on well-hydrated SiO_2 and that both contact angles of water and thicknesses of the monolayers were lower on the nonhydrated surfaces.³³ Le Grange et al. deposited OTS on hydrated and dehydrated substrates of fused silica.³⁶ They observed ordered, complete SAMs of OTS on hydrated substrates and decreased coverage compared to complete SAMs on dehydrated substrates. The interfacial film of water described by Brzoska et al. also decouples the silane film from the substrate, and several groups have shown that the density of siloxane bonds between the adsorbed silane film and substrate is small.^{36,38,39} The concentration of OH groups on the surface affects the mobility of the adsorbed OTS molecules.^{41,44} The OH groups act as nucleation and bonding sites for the formation of the monolayers. On mica substrates with very few OH groups, the OTS molecules are very mobile and can aggregate easily into ordered domains or "islands" before bonding to the substrate. On silicon substrates with many silanol groups, the OTS molecules have limited mobility and bond more quickly to the substrate. On these substrates, the OTS molecules adsorb more uniformly over the surface of the substrate and, initially, in a more disordered configuration.

The presence of water in the OTS solutions causes the OTS molecules to oligomerize in solution, and these oligomers have been shown to adsorb to surfaces more quickly than single molecules.^{35,52} The adsorption of these oligomers gives rise to the formation of well-ordered "islands" on surfaces in fractal patterns.^{35,53} With increasing deposition time, the gaps between islands are filled by other adsorbed islands and single molecules. The increased concentrations of water in the silane solution also increase the kinetics of adsorption of the silane molecules onto the substrate.^{34,40,44} Vallant et al. have shown that with decreasing concentrations of water, the growth of islands decreases and the formation of monolayers becomes more uniform.⁴⁴ Most studies of solution deposition of SA films of OTS are performed under ambient conditions where water levels are not controlled.

The orientation of adsorbed OTS molecules in the SA films can be compared using near edge X-ray absorption fine structure (NEXAFS) spectroscopy of the C 1s edge. In addition, quantitative comparisons can be made of the amount of adsorbed material in different SA films by determining the coverage from integration of the carbon absorption signal. NEXAFS spectroscopy has been used previously to study the structure of SAMs of alkanethiols on Au⁵⁴ and SAMs of OTS deposited under ambient air conditions.⁵⁵ In this paper, we use NEXAFS spectroscopy to study the orientation of adsorbed OTS molecules in SA films deposited under low-moisture conditions inside a drybox using two different lots of OTS that produced both ordered and disordered films under otherwise identical conditions. The orientation of OTS molecules in these films is compared to the orientation of OTS in a SAM deposited under ambient air conditions. The results from the NEXAFS spectroscopy are discussed in relation to measurements of advancing and receding contact angles of water and ellipsometric thickness of the SA films.

(40) Brunner, H.; Gibson, C. A.; Mayer, U.; Hoffmann, H. *Mikrochim. Acta* **1997**, 625.

(41) Brunner, H.; Vallant, T.; Mayer, U.; Hoffmann, H.; Basnar, B.; Vallant, M.; Friedbacher, G. *Langmuir* **1999**, *15*, 1899.

(42) Bierbaum, K.; Grunze, M.; Baski, A. A.; Chi, L. F.; Schrepp, W.; Fuchs, H. *Langmuir* **1995**, *11*, 2143.

(43) Britt, D. W.; Hlady, V. J. *Colloid Interface Sci.* **1996**, *178*, 775.

(44) Vallant, T.; Brunner, H.; Mayer, U.; Hoffmann, H.; Leitner, T.; Resch, R.; Friedbacher, G. *J. Phys. Chem. B* **1998**, *102*, 7190.

(45) Fadeev, A. Y.; McCarthy, T. J. *Langmuir* **2000**, *16*, 7268.

(46) Ulman, A. *Introduction to Ultrathin Organic Films from Langmuir–Blodgett to Self-Assembly*; Academic Press: San Diego, 1991.

(47) Cohen, S. R.; Naaman, R.; Savig, J. *J. Phys. Chem.* **1986**, *90*, 3054.

(48) Brzoska, J. B.; Shahidzadeh, N.; Rondelez, F. *Nature* **1992**, *360*, 719.

(49) Carraro, C.; Yauw, O. W.; Sung, M. M.; Maboudian, R. *J. Phys. Chem. B* **1998**, *102*, 4441.

(50) Davidovits, J. V.; Pho, V.; Silberzan, P.; Goldmann, M. *Surf. Sci.* **1996**, *352*, 369.

(51) Wang, R. W.; Wunder, S. L. *Langmuir* **2000**, *16*, 5008.

(52) Resch, R.; Grasserbauer, M.; Friedbacher, G.; Vallant, T.; Brunner, H.; Mayer, U.; Hoffmann, H. *Appl. Surf. Sci.* **1999**, *140*, 168.

(53) Doudevski, I.; Hayes, W. A.; Woodward, J. T.; Schwartz, D. K. *Colloids Surf., A* **2000**, *174*, 233.

(54) Hahner, G.; Woll, C.; Buck, M.; Grunze, M. *Langmuir* **1993**, *9*, 1955.

(55) Bierbaum, K.; Kinzler, M.; Woll, C.; Grunze, M.; Hahner, G.; Heid, S.; Effenberger, F. *Langmuir* **1995**, *11*, 512.

Experimental Section

Materials. Polished test grade silicon <100> wafers were purchased from Tygh Silicon. Octadecyltrichlorosilane ($\text{CH}_3(\text{CH}_2)_{17}\text{SiCl}_3$, 95%) was purchased from Gelest and was used as received. Toluene (99.8%, anhydrous) and chloroform (99+%, anhydrous) were purchased from Aldrich and were used without further purification. Ethanol (dehydrated, 200 proof) was purchased from Aaper Alcohol and Chemical Co and was used as received.

Deposition of Self-Assembled Organic Films. Silicon wafers were cleaved into pieces approximately $2\text{ cm} \times 2\text{ cm}$ and were cleaned by immersion in a piranha solution (7:3 (v/v) of 98% H_2SO_4 :30% H_2O_2) at 90°C for 30 min. The silicon pieces were immediately rinsed with deionized water (resistivity $\geq 18\text{ M}\Omega\text{-cm}$.) several times and were blown dry with nitrogen. Clean substrates were immersed in 0.1% (v/v) solutions of OTS in toluene. Silane depositions were performed in either a drybox with a nitrogen atmosphere (Vacuum Atmospheres, dew point $< -60^\circ\text{C}$) or in ambient air. For silane depositions performed in the drybox, substrates were removed from OTS solutions after deposition times between 4 and 96 h. For silane depositions performed in ambient air, substrates were removed from OTS solutions after 30 min. After the substrates were removed from the silane solution, they were rinsed with chloroform and absolute ethanol and were dried under a stream of nitrogen.

Measurement of Contact Angles. Advancing and receding contact angles of deionized water were measured on the SA films at ambient temperature using a Future Digital Scientific model OCA15 video contact angle system. Contact angles were measured on the opposite edges of at least three drops and averaged. The values were reproducible to within 1.3° .

Ellipsometry Measurements. Ellipsometry measurements were made on a Rudolf Research/Auto EL II ellipsometer using He-Ne Laser ($\lambda = 632.8\text{ nm}$) at an incident angle of 70° relative to the surface normal of the substrates. The thicknesses of the SA films and the oxide layer cannot be measured simultaneously, and at least three separate spots were measured on each substrate before and after deposition of the SA film to determine the thickness of the oxide layer and the thickness of the SA film plus the oxide layer. The thickness of the oxide layer of silicon wafers was typically 17 \AA . A refractive index of 1.45 was used for calculation of the thicknesses of the SA films and the oxide.

NEXAFS Measurements. NEXAFS spectroscopy was performed at the Synchrotron Radiation Center (SRC) on the HERMON beam line (port 033). Absorption spectra were taken at the C 1s edge for the SA films. The photon energy was scanned, and the sample photocurrent was recorded as a measure of the absorption cross section. The light was at least 90% linearly polarized, and for each sample scans were taken at various angles between the polarization vector and the sample normal ranging from 90° (normal incidence) to 20° (grazing incidence). NEXAFS spectra of molecules containing hydrocarbon chains at the C 1s edge are dominated by a sharp resonance at 287.7 eV , labeled as R^* , that has been attributed to excitations to Rydberg states. A second, broader resonance at 293.1 eV has been attributed to excitations to C-C σ^* orbitals.^{56,57} The energy region for the C 1s edge was chosen between 280 and 315 eV. Spectra were normalized to a clean gold reference signal evaporated in situ on silicon to remove the transmission function of the optics. In addition, all spectra were normalized to a mesh signal measured concurrently to remove beam fluctuations. Except when calculating absolute coverages, the signal below the carbon 1s absorption edge was normalized to one to remove differences in the absorption depth at different angles. The electron yield is proportional to the electron escape depth over the absorption length, thereby changing with the angle of incidence. After every few scans the light spot on the sample was moved to prevent extended exposure to photons and any resulting radiation damage.

Table 1. Advancing (θ_A) and Receding (θ_R) Contact Angles of Water, Ellipsometric Thickness, and Photoemission Coverage of SA Films of OTS at Different Times of Deposition

reagent	deposition time (h)	θ_A ($^\circ$)	θ_R ($^\circ$)	thickness (\AA)	photoemission coverage (A.U.)
OTS-1	6	100 ± 1	79 ± 1	22 ± 2	0.46 ± 0.02
	22	107 ± 1	93 ± 1	27 ± 1	0.62 ± 0.02
	48	109 ± 1	95 ± 3	29 ± 2	0.74 ± 0.02
	96	111 ± 1	100 ± 3	26 ± 1	0.78 ± 0.02
OTS-2	4	80 ± 2	28 ± 1	12 ± 1	0.13 ± 0.02
	24	92 ± 1	29 ± 1	19 ± 1	0.21 ± 0.02
	31	102 ± 1	41 ± 1	24 ± 1	0.34 ± 0.02
	48	104 ± 2	66 ± 1	43 ± 1	0.69 ± 0.02

Results and Discussion

In these experiments, conditions were chosen to be similar to experimental conditions that we^{6-8,12,58} and others³⁰⁻³² have used previously to deposit SA films of OTS. In the previous experiments, the conditions were chosen for ease of sample preparation while maintaining the desired properties of the SA films. We routinely perform kinetic studies of the depositions to monitor contact angles and ellipsometric thickness. These studies are performed to ensure that our deposition conditions produce SA films with the desired properties. Depositions were performed in the drybox to eliminate the formation of polymeric siloxane that forms on the surface of the substrate as a white, cloudy film that generally results during depositions performed in ambient conditions. The substrates were assumed to be well hydrated as piranha-cleaned Si/SiO_x is a hydrophilic surface and maintains an interfacial water layer even inside the drybox. Solvents and OTS were used as received, and the deposition temperature and concentration of water in silane solutions were not controlled.

For this paper, SA films of OTS were deposited from solution under both ambient air conditions and low-moisture conditions in a drybox. Three different lots of OTS (purchased over an eight-month period) were used to make silane solutions in toluene. For depositions in the drybox, OTS from two different lots was used to make silane solutions. OTS-1 was purchased and opened first, and OTS-2 was purchased and opened approximately eight months later. Both OTS-1 and OTS-2 were opened only within the drybox and were sealed between uses. We were unable to discern any chemical difference or the presence of contaminants in OTS-1 and OTS-2 using ^1H and ^{13}C nuclear magnetic resonance spectroscopy. The two reagents OTS-1 and OTS-2 yielded SA films with different characteristics when deposited under the same experimental conditions. A more exhaustive investigation has not been performed to determine the origin of the differences. For OTS films deposited in ambient air, a third bottle of OTS (OTS-air) was used that had been opened to air many times.

Advancing and receding contact angles and thicknesses of OTS films with increasing deposition times for OTS-1 and OTS-2 are listed in Table 1. For films grown from OTS-1 and OTS-2, advancing and receding contact angles and thickness increased with increasing deposition time, indicative of increasing coverage of alkane chains on the surface. For the SA film grown from OTS-air, the advancing and receding contact angles equaled $110^\circ \pm 1^\circ$ and $100^\circ \pm 1^\circ$, respectively, and the thickness was $26 \pm 2\text{ \AA}$. These values agreed well with reported values for well-ordered SAMs of OTS.^{30,32,37,59} For OTS-1 after 96 h, the

(56) Bagus, P. S.; Weiss, K.; Schertel, A.; Woll, C.; Braun, W.; Hellwig, C.; Jung, C. *Chem. Phys. Lett.* **1996**, *248*, 129.

(57) Schertel, A.; Hahner, G.; Grunze, M.; Woll, C. *J. Vac. Sci. Technol., A* **1996**, *14*, 1801.

(58) Peters, R. D.; Yang, X. M.; Kim, T. K.; Nealey, P. F. *Langmuir* **2000**, *16*, 9620.

values for the contact angles and thickness were equal to the values for OTS-air indicating a close-packed methyl-terminated surface for both films. For OTS-2 after 48 h, the advancing contact angle was 104° , 6° less than the advancing contact angle for OTS-air, and the receding contact angle was 66° , 34° less than the receding contact angle for OTS-air. The ellipsometric thickness for OTS-2 after 48 h was 43 \AA , 17 \AA larger than the thickness for OTS-air.

Polarization-dependent X-ray absorption spectroscopy allows comparison of the orientation of molecules within a SA film. The dipole approximation to the transition matrix element between an s-like core level and an empty state is proportional to $\cos^2\theta$, where θ is the angle between the transition dipole moment and the polarization vector of the light. To study the orientation of the molecules within a SA film of OTS, changes in the R^* and $C-C \sigma^*$ resonant intensities are measured as a function of the angle of incidence of the light. For OTS in an all-trans conformation, the average $C-C$ bond direction defines a molecular axis along the chain, and the average $C-H$ bond direction is perpendicular to this axis. The average transition dipole moments for the $C-C \sigma^*$ and R^* resonances share this symmetry. For a completely disordered sample with a larger number of gauche defects, no polarization-dependent changes will be observed. For a well-ordered monolayer, the molecules will be packed nearly vertically in an all-trans conformation with an average tilt of the molecular axis from the normal and a random azimuthal distribution. Therefore, when the polarization vector is normal to the surface (grazing incidence), the $C-C \sigma^*$ resonance will be maximum and the R^* will be minimum, and conversely when the polarization vector is parallel to the surface (normal incidence), the $C-C \sigma^*$ resonance will be minimum and the R^* resonance will be maximum.

Figure 1 shows NEXAFS spectra for SA films of OTS-1 and OTS-2 at deposition times ranging from 4 to 48 h. For each deposition time, NEXAFS spectra at incidence angles θ of 45° and 90° are shown. The two primary features are characteristic of alkane molecules and agree with earlier assignments of transitions from the $C 1s$ core level to the unoccupied Rydberg and $C-C \sigma^*$ orbitals. For OTS-1 with a deposition time of 6 h, no change in the intensities of the R^* and $C-C \sigma^*$ resonances was observed with θ . This lack of polarization dependence showed the adsorbed alkyl chains had no preferred orientation and contained a high density of gauche conformations. With increasing deposition time, these resonances began to exhibit increasing polarization dependence. For deposition times of 22 and 48 h, the intensity of the R^* resonance increased as θ changed from 45° to 90° , and the intensity of the $C-C \sigma^*$ resonance decreased as θ changed from 45° to 90° . This polarization dependence was evidence for an increase in trans conformations for the adsorbed alkyl chains. OTS-1 initially adsorbed to the surface as a disordered film but exhibited increasing order with increasing deposition time. For OTS-2, no polarization dependence for the intensities of the R^* and $C-C \sigma^*$ resonances was observed for any deposition time up to 48 h. The adsorbed molecules in these films showed no preferred orientation, and these films remained disordered with increasing deposition time.

The SA film of OTS-1 with a deposition time of 96 h was identical to the SAM of OTS-air on the basis of contact angle measurements and ellipsometric thickness. NEXAFS spectra comparing the SA film of OTS-1 with a

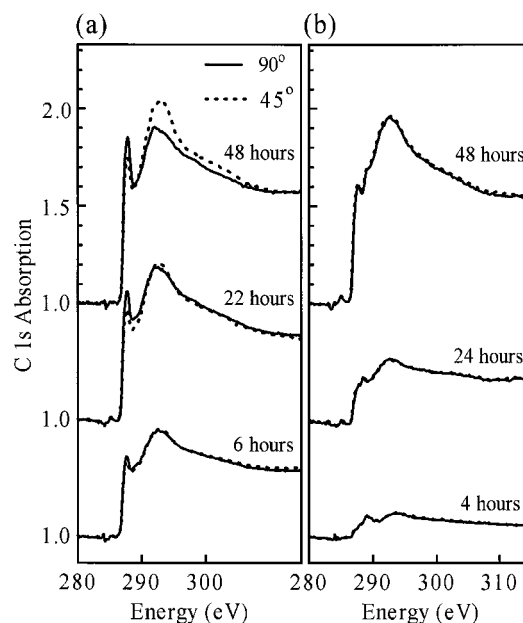


Figure 1. Series of NEXAFS spectra for SA films of (a) OTS-1 and (b) OTS-2 for deposition times ranging from 4 to 48 h. For every deposition time in both (a) and (b), spectra at angles of incidence of 45° and 90° are shown. The spectra for different deposition times are offset for clarity. For OTS-1, the increase in the polarization dependence of the $C-C \sigma^*$ and $C-H$ orbitals with increasing time was evidence for an increase in trans conformations of the adsorbed alkyl chains. In contrast, for OTS-2 there is no polarization dependence indicating that the SA films remain disordered.

deposition time of 96 h and the SAM of OTS-air are shown in Figure 2. For both OTS-1 and OTS-air, the intensity of the R^* resonance increased with increasing θ from 20° to 90° , and the intensity of the $C-C \sigma^*$ resonance decreased with increasing θ from 20° to 90° . This polarization dependence clearly demonstrated a high density of trans conformations for the adsorbed alkyl chains in both films. However, the magnitude of the polarization-dependent effects is clearly smaller in OTS-1 suggesting possible structural differences between the two films.

Computing the average tilt of the adsorbed molecules with respect to normal gives a more quantitative comparison of the films' structure. The average tilt is most easily computed from difference spectra between the NEXAFS spectra at different polar angles as outlined by Schertel et al.^{56,57,60} The primary advantage to this approach is that the exact shape and position of the absorption edge and other nonpolarization dependent features are removed by the subtraction leaving only the polarization-dependent resonances of interest. Assuming a random azimuthal distribution, the resonance intensities in the difference spectra depend on the polar angles as

$$I = C(1 - 3/2 \sin^2 \alpha)(\cos^2 \theta - \cos^2 \theta_1)^{61} \quad (1)$$

Here, the parameter α describes the average tilt of the orbital with respect to the surface normal, θ_1 is the reference polar angle, and C is a constant. By using a reference film with known tilt, the constant C for a specific resonance can be determined and subsequently applied to find the average tilt for a different film of the same

(59) Tillman, N.; Ulman, A.; Schildkraut, J. S.; Penner, T. L. *J. Am. Chem. Soc.* **1988**, *110*, 6136.

(60) Kinzler, M.; Schertel, A.; Hahner, G.; Woll, C.; Grunze, M.; Albrecht, T.; Holzhutrer, G.; Gerber, T. *J. Chem. Phys.* **1994**, *100*, 7722.

(61) Stohr, J. *NEXAFS Spectroscopy*; Springer-Verlag: New York, 1992.

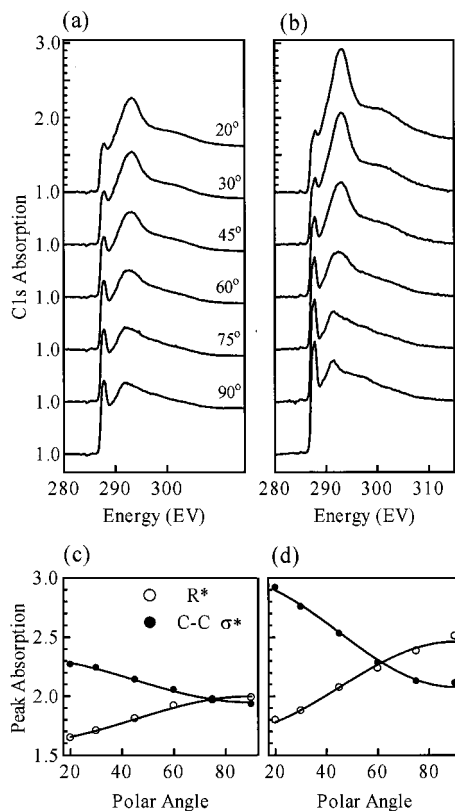


Figure 2. Series of NEXAFS spectra for different angles of incidence ranging from 20° to 90° for (a) SA film of OTS-1 with a deposition time of 96 h and (b) SAM of OTS-air. The spectra at different angles of incidence are offset for clarity. For both films the C–C σ^* resonance is excited preferentially at grazing incidence while the C–H is excited preferentially at normal incidence, indicating a high density of trans conformations in the two films.

molecule. The linear polarization factor of the light and the transition probability do not have to be considered explicitly.

Figure 3a and b show difference spectra for OTS-1 and OTS-air derived from the spectra in Figure 2. In each case, the spectrum at 90° is used as a reference and the differences at polar angles from 20° to 75° are taken with respect to this reference. The three features that exhibit polarization dependence are fit with Gaussians at energies of 287.6, 293.2, and 301.0, in good agreement with earlier assignments.^{54,55} The peak areas for the R* and C–C σ^* resonances for OTS-1 and OTS-air are plotted in Figure 3c and d along with best fits of function (1). The SAM of OTS-air was taken as a control with $\alpha = 15^\circ$, yielding values of C for the two resonances. These values of C were used to determine the average tilt angle for the chains in the SA film of OTS-1. Separate calculations for the R* and C–C σ^* resonances yielded values of α of 38° and 38.3°, respectively. The higher value of α for OTS-1 was due to either a lower-packing density of adsorbed chains causing the molecules to tilt to fill voids or to a higher density of gauche conformations.

Photoemission coverages for the SA films of OTS-1 and OTS-2 were determined from the NEXAFS spectra at 45°. To calculate absolute coverage, the signal below the C 1s absorption edge was not normalized to one. Instead, a linear background was extrapolated from the pre-edge region and subtracted, and then the remaining signal due entirely to C 1s absorption was integrated. Since the thickness of the OTS monolayers is less than the escape depth of the electrons, this total integrated intensity

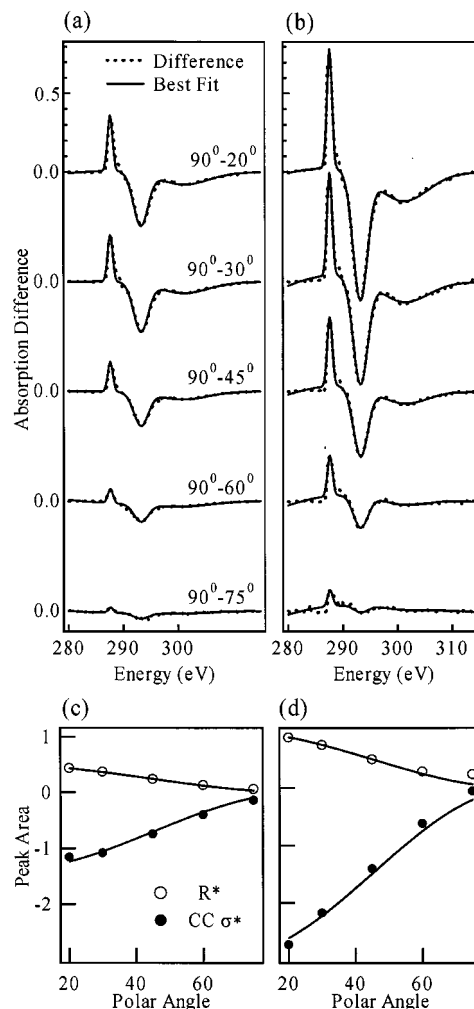


Figure 3. Difference spectra of normal incidence and angles of incidence ranging from 20° to 75° for (a) SA film of OTS-1 with deposition time of 96 h and (b) SAM of OTS-air. The three primary features for each spectra are fit with Gaussians, and the resulting difference intensities for the C–H and C–C σ^* resonances are plotted as a function of angle in (c) and (d). Fits to the difference intensities are used to determine the average tilt of the alkane chains, a quantitative measure of the extent of ordering within the film. An average tilt of 38° is computed for OTS-1 assuming an average tilt of 15° for OTS-air.

should be directly proportional to the coverage of carbon. Stohr reports a magic polar angle of 55° at which the orientation and ordering of the molecules on the surface will not affect the intensity of the resonances.⁶¹ By comparing spectra at a fixed angle of 45°, most of the modulations due to polarization dependence and other angular dependence should be removed. The coverage values were normalized to the photoemission coverage for the SAM of OTS-air calculated similarly from a NEXAFS spectrum at 45°. The normalized values for photoemission coverage are listed in Table 1. For OTS-1, 80% of the final coverage at 96 h was achieved after 22 h of deposition. For OTS-2, 80% of the final coverage at 48 h was not achieved until after 31 h of deposition.

Grunze and co-workers have studied the growth of SA films of both alkylsiloxanes⁵⁵ and alkanethiols⁵⁴ using NEXAFS spectroscopy. They deposited alkylsiloxanes of OTS and propyltrichlorosilane (PTS) on Si/SiO₂ in ambient air conditions similar to depositions of OTS-air such that the deposition process was on the order of minutes as opposed to hours for depositions performed in the drybox for OTS-1 and OTS-2.⁵⁵ Using NEXAFS spectroscopy, they

determined average tilt angles for the adsorbed chains in the SA films. Because of no polarization dependence in the NEXAFS spectra, SA films of PTS were concluded to be disordered with no preferred orientation for the adsorbed molecules. For OTS, they observed ordered films for deposition times ranging from 15 s to 24 h. After 15 s, α was 40° , and after 5 min, α decreased to 28° . For 24-h deposition, they observed an average tilt angle less than 10° . They concluded that the partial ordering ($\alpha = 40^\circ$ at 15 s and $\alpha = 28^\circ$ at 5 min) for incomplete films of OTS suggested island growth. The decrease in α with increased deposition time, that is, the increase in the order of the films with increased deposition time, was due to a slow ordering process where the chains undergo a transition to an all-trans conformation because of van der Waals interactions between chains. The SA films of PTS did not undergo this ordering transition because the PTS chains were too short and the van der Waals interactions were too small to induce ordering. For alkanethiols on Au, they observed two stages of growth of the SA films.⁵⁴ In the first stage for deposition times on the order of 10 min, the alkanethiols adsorbed to the surface in a uniform, disordered manner that followed Langmuir adsorption kinetics. During the second stage with deposition times on the order of hours, the films became more dense and ordered as the coverage approached that of a complete SAM and α equaled 35° . During this second stage as the density of the SA film increased, the adsorbed chains underwent conformational changes leading to chain stretching and increased order. The adsorption in the second stage has a longer time constant than in the first stage. Bain et al. also have reported a two-stage growth process for alkanethiols on Au where the second stage has a longer time constant than the first stage.⁶² Generally, the films achieve $\sim 80\%$ of the final coverage within the first stage and undergo additional adsorption and reorientation of the adsorbed chains during the second stage to reach the final coverage and film thickness.

The growth of SA films of OTS-1 was similar to the growth of alkanethiols on Au as observed by Hähner et al. Two stages of growth were also apparent. In the first stage up to 22 h, the chains adsorbed uniformly over the surface with no or little preferred orientation, and the films were disordered with coverages less than $\sim 80\%$ of the final coverage. In the second stage from 22 to 96 h, the final 20% of the total coverage was achieved, and the extent of ordering (the polarization dependence of the intensities of the C–H and C–C σ^* resonances in the NEXAFS spectra) increased with increasing deposition time over a much longer time period than observed for the first stage. The similarity between the growth of films of OTS-1 and alkanethiols suggests that the SA films of OTS-1 deposited in the drybox grew in a uniform manner. Initially, the chains were disordered on the surface, and with increased deposition time, the density of the film increased such that van der Waals interactions between chains became strong enough to induce an ordering transition to an all-trans conformation. This growth mechanism agrees with the uniform model for growth of SAMs of OTS as discussed in the Introduction.

OTS-air exhibited much faster kinetics of adsorption than OTS-1. For OTS-air, a complete SAM was deposited in 30 min, similar to the times observed by Bierbaum et al.⁵⁵ For OTS-1 after 96 h, a SA film with only 78% of the final coverage of the SAM of OTS-air had been deposited although the contact angles and ellipsometric thicknesses

were equal for the two films. This difference in coverage and the different values of α for the two films were due to the different deposition conditions for the two films. The absorption of water from the atmosphere into the silane solution resulted in faster adsorption kinetics for the OTS molecules^{34,40,44} most likely because of oligomerization or polymerization of OTS molecules that also increased the adsorption kinetics.^{35,52} For OTS-air, the growth of the SAM most likely followed the island growth mechanism. OTS-1 followed a uniform, two-stage growth mechanism.

The different coverages and values of α for the films of OTS-air and OTS-1 suggest that there may be an inherent difference between the structures of films that grow following different growth mechanisms. The SA film of OTS-1 that grew following the uniform mechanism exhibited an α of $\sim 38^\circ$. SAMs of OTS that grow as coalescing islands have been reported to have an α of 10 to 17° .^{28,46,55} SAMs of OTS deposited using the Langmuir–Blodgett (LB) method were reported to have an α of ~ 8 to 10° .²⁸ These different values of α that depend on the growth mechanism suggest a limitation in the ordering process that is related to chain mobility; decreased mobility due to grafting decreases the extent of ordering by introducing steric hindrances to the insertion of additional chains into a nearly complete film. In the LB technique, the silane molecules self-assemble on water and are mechanically compressed in the LB trough. The chains are mobile because they are not grafted to any surface, and they can rearrange themselves to become more tightly packed. For island growth, a large cluster of molecules adsorbs to the surface with only a few surface-island bonds grafting the island to the substrate, and the molecules in this cluster can rearrange to become more tightly packed. This mobility, however, is limited to chains within a cluster. Once islands coalesce, further rearrangement and ordering cannot occur. For uniform growth, single chains adsorb to the surface. A higher density of surface grafts is more likely for uniform growth than for island growth because individual chains adsorb to the surface and may or may not bond with adjacent chains to form a siloxane network. This increased density of surface grafts results in lower mobility for the adsorbed chains. Therefore, as the density of the film increases and van der Waals interactions induce the ordering process, this process is limited by the inability of the molecules to diffuse along the surface to accommodate additional molecules and reach the tightest packing configuration. We believe the higher value of α for OTS-1 compared to OTS-air is due to a lower packing density and not to an increased density of gauche conformations. The smaller photoemission coverage for OTS-1 compared to OTS-air is indicative of this reduced density.

One of the most interesting results from this study is the comparison of the ellipsometric thickness to the photoemission coverage. As can be seen from the data in Table 1, the ellipsometric thickness did not correlate well with the photoemission coverage. For several films, we measured thicknesses between 22 and 29 Å; however, for all of these films, the photoemission coverage was significantly less than that for the SAM of OTS-air. Assuming an all-trans conformation and $\alpha = 38^\circ$, we calculated a thickness of ~ 20.6 Å for OTS-1 with a deposition time of 96 h. This thickness is $\sim 79\%$ of the thickness of OTS-air which is comparable to the percentage of photoemission coverage of OTS-1 to OTS-air. For the ellipsometry measurements, we assumed a constant index of refraction of 1.45 as has been used previously.^{30,31} This index of refraction is valid under the assumption of a close-

(62) Bain, C. D.; Troughton, E. B.; Tao, Y. T.; Evall, J.; Whitesides, G. M.; Nuzzo, R. G. *J. Am. Chem. Soc.* **1989**, *111*, 321.

packed, quasi-crystalline film that is comparable to a liquid or solid hydrocarbon film. For the films of OTS-2 especially, this index of refraction is likely not valid as these films are disordered and have densities that differ from quasi-crystalline films. The ellipsometric thickness alone is not the best characterization technique for use as an indicator to determine completeness of deposition for these disordered films or for comparing SA films that were deposited under different conditions. A technique such as X-ray reflectivity that measures thicknesses directly and does not rely on assumed film properties is better suited to measure the thicknesses of disordered films.

In contrast to the ellipsometric thickness, the receding contact angle does appear to be more sensitive to the density of trans conformations and the packing of methyl groups at the surface of the SA films. We estimate a reduced density for the SA films by dividing the photoemission coverage by the ellipsometric thickness. The values for the receding contact angles in Table 1 correlate well with this reduced density. This correlation suggests that the receding contact angle is sensitive to the packing of the adsorbed molecules in the SA film. All films of OTS-2 were found to be disordered from the NEXAFS spectra shown in Figure 1b, and θ_R for all of these films was less than 66° . For OTS-1, θ_R was greater than 79° for all deposition times, even after only 6 h. After 22 h where a polarization dependence in the NEXAFS scans was observable, θ_R was greater than or equal to 93° . The receding contact angle appears to be more sensitive to the structure of the SA film than both the advancing contact angle and ellipsometric thickness, but the receding contact angle is used less often than the advancing contact angle and ellipsometric thickness to characterize SA films. A large hysteresis between the advancing and receding contact angles may be due to surface roughness or chemical heterogeneity that both imply poor packing of the adsorbed chains (high density of gauche conformations) resulting in voids or in the presence of methylene groups at the surface. A discrepancy does exist, however, when comparing the structures of the SA film of OTS-1 with a deposition time of 96 h and the SAM of OTS-air, where each film has a receding contact angle of 100° . The coverages and α 's of these two films were not equal; thus, the receding contact angle does not give complete information regarding the structure of the film. We believe the receding contact angle

is indicative of the density of trans conformations and the packing of methyl groups at the surface of the film. An all-trans conformation will result in a close-packed methyl-terminated surface giving the highest values for the contact angles and the least hysteresis. On the basis of the NEXAFS spectra in Figure 1, a receding contact angle greater than 93° is indicative of a mostly close-packed methyl surface with at least partial ordering into an all-trans conformation. A receding contact angle of 100° is indicative of a close-packed methyl-terminated surface with the adsorbed chains in an all-trans conformation. The receding contact angle is not indicative of the total packing density and the average tilt angle of adsorbed chains.

Conclusions

The structure of SA films of OTS was studied using a combination of advancing and receding contact angle measurements, ellipsometry, and NEXAFS spectroscopy. A series of SA films that exhibited increasing order with increasing deposition time and a series of SA films that remained disordered for all deposition times were studied. The structure of the SA films was determined by examining the polarization dependence of the NEXAFS spectra. SA films of OTS deposited in the drybox were found to grow following the uniform mechanism. Comparing the SA film of OTS-1 with a deposition time of 96 h to the SAM of OTS-air, α for OTS-1 was greater and the photoemission coverage for OTS-1 was smaller than for the SAM of OTS-air. These differences are due to a lower packing density for OTS-1 compared to OTS-air. The receding contact angle was found to be correlated better with the photoemission coverage than either the advancing contact angle or ellipsometric thickness.

Acknowledgment. Funding for this work was provided by the Semiconductor Research Corporation (Grant Number 98-LP-452), NSF Career Award (Grant Number CTS-9703207), and the Camille Dreyfus Teacher-Scholar Awards Program. Facilities were supported by DARPA/ONR (Grant Number N00014-97-1-0460) and the NSF (Grant Number DMR-0084402). The Synchrotron Radiation Center at the University of Wisconsin-Madison is supported by the NSF under Award No. DMR-9531009.

LA011198J